Finding turning-points in ultra-high-resolution animal movement data

Jonathan R. Potts[1,a], Luca Börger[2], D. Michael Scantlebury[3], Nigel C. Bennett[4,5], Abdulaziz Alagaili[5], Rory P. Wilson[2]

Short title: Turning-point algorithm

Key words: Animal movement, Behaviour, Biologging, Change point, High-resolution data, Movement ecology, Turning point

1 School of Mathematics and Statistics, University of Sheffield, Hicks Building, Hounsfield Road, Sheffield, UK, S3 7RH

a E-mail: j.potts@sheffield.ac.uk

2 Department of Biosciences, College of Science, Swansea University, Singleton Park, Swansea, SA2 8PP, UK

3 School of Biological Sciences, Institute for Global Food Security, Queens University Belfast, Belfast BT9 7BL, UK

4 Department of Zoology and Entomology, University of Pretoria, Pretoria 0002, South Africa

5 Zoology Department, King Saud University, P.O Box 2455, Riyadh 11451, Saudi Arabia

Abstract

1. Recent advances in biologging have resulted in animal location data at unprecedentedly high temporal resolutions, sometimes many times per second. However, many current methods for analysing animal movement (e.g. step selection analysis or state-space modelling) were developed with lower-resolution data in mind. To make such methods usable with high-resolution data, we require techniques to identify features within the trajectory where movement deviates from a straight line.

2. We propose that the intricacies of movement paths, and particularly turns, reflect decisions made by animals so that turn points are particularly relevant for behavioural ecologists. As such, we introduce a fast, accurate algorithm for inferring turning-points in high-resolution data. For analysing big data, speed and scalability are vitally important. We test our algorithm on simulated data, where varying amounts of noise were added to paths of straight-line segments interspersed with turns. We also demonstrate our algorithm on data of free-ranging oryx (*Oryx leucoryx*). We compare our algorithm to existing statistical techniques for breakpoint inference.

3. The algorithm scales linearly and can analyse several hundred-thousand data-points in a few seconds on a mid-range desktop computer. It identified turnpoints in simulated data with complete accuracy when the noise in the headings had a standard deviation of $\pm 8^{\circ}$, well within the tolerance of many modern biologgers. It has comparable accuracy to the existing algorithms tested, and is up to three orders of magnitude faster.

4. Our algorithm, freely available in `R` and `Python`, serves as an initial step in processing ultra high-resolution animal movement data, resulting in a rarefied path that can be used as an input into many existing step-and-turn methods of analysis. The resulting path consists of points where the animal makes a clear turn, and thereby provides valuable data on decisions

underlying movement patterns. As such, it provides an important breakthrough required as a starting point for analysing sub-second resolution data.

1 Introduction

Animal movement is a key process underlying many ecological systems (Nathan et al., 2008; Kays et al., 2015; Hays et al., 2016). Until recently, our understanding of the drivers of movement was limited by the resolution of data obtainable by technologies such as global positioning systems (GPS) and Argos telemetry (Johnson et al., 2002; Jerde and Visscher, 2005; Hurford, 2009; McClintock et al., 2015). However, technological advances, particularly regarding accelerometers and magnetometers, have enabled tracks to be constructed at extremely high resolutions (Wilson et al., 2008; Brown et al., 2013; Noda et al., 2014; Walker et al., 2015; Bidder et al., 2015; Williams et al., 2017). Indeed, often the time interval between consecutive locations is shorter than the time it takes for an animal to travel a distance equal to its body length, so that the movement data is, for all practical purposes, continuous (Wilmers et al., 2015).

Whilst such data open up a wealth of opportunity for better understanding of animal movement, many of the existing mathematical and statistical techniques for analysing location data were developed with older, coarser data in mind. As such, they often fail to scale-up to the new world of big, high-resolution data: techniques that work well on 1,000s of data points gathered at hourly intervals may be very different to those required to analyse 1,000,000s of data points at a resolution of 10Hz.

For example, many highly successful techniques, such as state-space modelling (Morales et al., 2004; Jonsen et al., 2005; Patterson et al., 2008) and step selection analysis (Fortin et al., 2005; Rhodes et al., 2005; Forester et al., 2009; Avgar et al., 2016), were formulated for data where there is reasonable chance of finding interesting behavioural information in each 'step' between successive data points. Yet, if the datapoints are only a fraction of a second apart, the resulting information is minimal, and it is necessary to find points that correspond to

the animal doing something more interesting than simply carrying-on in the same straight-line trajectory.

Consequently, for high-resolution data, we need techniques that can infer when the animal is making a turn. The idea of examining animal paths as 'steps and turns' has been at the heart of movement ecology for several decades (Kareiva and Shigesada, 1983; Bovet and Benhamou, 1988; Turchin et al., 1991; Turchin, 1998) in various forms, including step selection analysis, biased correlated random walks (Codling et al., 2008), many state-space models, and even continuous-time models (Parton et al., 2016). So to apply such 'step and turn' modelling techniques to modern, ultra-high resolution data, we need a way of rapidly and accurately inferring the turning points in the data-stream.

The aim of this paper is to provide such a technique. The idea is to view the path as a stream of *headings* of the animal, rather than locations. We then look for switches in the heading by sliding a small window across the path and observing where the standard deviation across the window spikes (Fig. 1). This indicates a turn. If required, we can further post-process the data by removing 'small' turning angles, that are not deemed to be indicative of an actual behavioural decision. The resulting algorithm scales linearly with the length of the data stream, and can process 100,000s of data points in a few seconds on a mid-range desktop (Intel i7 2.5GHz processor).

This algorithm leads to a description of the animal's movement in terms of straight-line segments interspersed with turns, giving a biologically meaningful summary of the animal's movement behaviour whereby the turns are likely to represent actual decisions of the animal. This contrasts with many studies involving lower-resolution data, where the turns are implicitly assumed to occur precisely at the points where the locations were measured (Morales et al., 2004; Fortin et al., 2005; Avgar et al., 2016) [but see Turchin et al. (1991); Codling and Plank (2011), mentioned in more detail below]. Therefore, combined with high-resolution data, our algorithm opens the door to more biologically accurate application of popular techniques for analysing 'move and turn' data, such as step selection analysis and state space models.

To test the efficacy of our algorithm, we use a combination of simulated and real data. For the simulations, we construct paths of straight-line segments joined together by sharp turns, then add varying amounts of noise, to reflect both the error inherent in data-gathering technologies and the noise arising from animal locomotion (e.g. small 'rocking' movements of the sensor due to the animal's gait, or avoidance of small obstacles like rocks). This enables us to analyse the accuracy of our algorithm in inferring the correct turning points. We then use data on free ranging oryx to demonstrate how to apply the technique to a real-world scenario.

Ours is not the first algorithm to segment data into straight lines and turns. Turchin et al. (1991) developed a method that has proved popular in movement ecology for a number of years. An alternative method was later put forward by Codling and Plank (2011). However, these methods were both designed for the sort of low-resolution data that has historically been available, and we show here that they do not perform so well with higher resolution data. Away from movement ecology, several sophisticated and general techniques have been developed to segment data streams, mainly concerned with studying DNA sequences [e.g. Picard et al. (2005); Erdman and Emerson (2008); Franke et al. (2012); Rivera and Walther (2013)]. These have the advantage of being well-grounded in statistical theory. The best-performing technique [pruned dynamic programming, according to Hocking et al. (2013)] has also been written into a flexible and convenient `R` package, called `Segmentor3IsBack` (Cleynen et al., 2014). However, when we applied this algorithm to data, it was typically 10^3 times slower than ours, which could cause it to be prohibitively slow for very long data streams.

In summary, we describe here a fast, light-weight algorithm for inferring turning points in high-resolution animal movement data. We hope that this will enable more sophisticated use of step-and-turn analysis techniques, where the turns are more closely related to the underlying behavioural decisions of the animal (Wilson et al., 2013).

2 Methods

2.1 The turning-point algorithm

We describe an algorithm to be used on data of animal *headings*. This contrasts with many animal movement studies which focus on *locational* (or positional) data. The reasons for this are that (a) high resolution data tends to arrive from magnetometers that record headings rather than locations, and (b) headings are the natural parameter for determining turning points (TPs).

The essence of the algorithm is contained in the following two steps. First, we slide a window across a time-series of headings and looking for places where the squared circular standard deviation (SCSD) across that window spikes. The SCSD is a measure of the 'spread' of angles, and is used in place of the variance to account for the circular nature of angular distributions. Note that we choose not to use the term 'circular variance' as, in circular statistics, this is not consistently defined and may not be the square of the circular standard deviation [see e.g. Berens (2009)]. The spikes in SCSD indicate that the animal has turned. Second, we refine the set of candidate TPs by rejecting those that are below some threshold value.

To describe the algorithm precisely, we need to introduce some notation. Let $h_1, \ldots, h_N$ be a time series of headings for the animal, collected at evenly-spaced time-points $t_1, \ldots, t_N$. Consider a small time window, W, about each data point and calculate the SCSD, s_i, of the heading across this window. In other words, s_i is the SCSD of $\{h_{i-W/2}, \ldots, h_{i+W/2}\}$ for each time-point t_i where $i \in \{1 + W/2, \ldots, N - W/2\}$ (W must be an even number). The SCSD is given by the following formula

$$s_i = \ln\left(\frac{1}{\bar{R}_i^2}\right), \tag{1}$$

where $\bar{R}_i = \sqrt{\overline{\sin(h_i)}^2 + \overline{\cos(h_i)}^2}$, $\overline{\sin(h_i)}$ is the average of $\{\sin(h_{i-W/2}), \ldots, \sin(h_{i+W/2})\}$, and $\overline{\cos(h_i)}$ is the average of $\{\cos(h_{i-W/2}), \ldots, \cos(h_{i+W/2})\}$. The SCSD copes with the fact that

$0° = 360°$, which stops us from using the usual definition of 'standard deviation'.

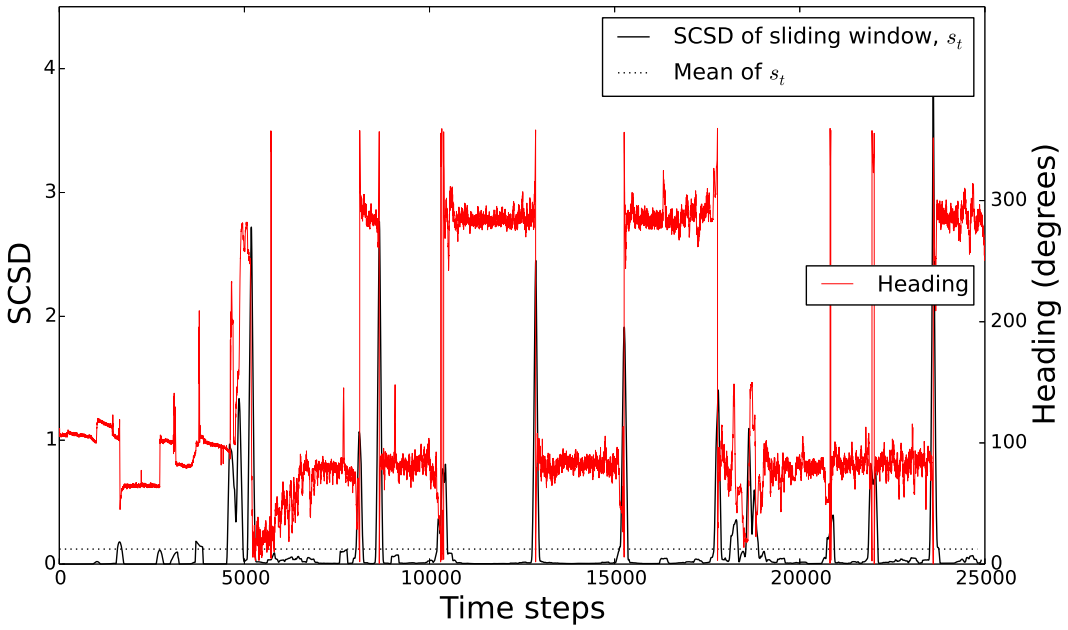

Fig. 1. Method for inferring turning points from circular standard deviation. The red curve gives the recorded headings of an example oryx, measured at 40Hz resolution. The squared circular standard deviation (SCSD) of the heading across a sliding window of size $W = 200$ data points is given by the black curve. Where this spikes above the mean SCSD, we infer that a turn might have taken place. We then do a second check to see that the heading has changed by more than a given threshold angle θ_{thresh} (see Main Text for more details). For example, this removes the points misidentified as turns at around timesteps 21,000 and 22,000.

The value of s_i will 'spike' when the animal turns sharply. We use these spikes to infer changes in the direction of the animal's movement (Figure 1). More precisely, a *spike* in the time series, $\{s_{1+W/2}, \ldots, s_{N-W/2}\}$, of SCSDs is defined to be a contiguous set of points, $\{s_i, \ldots, s_{i+k}\}$, each of which is greater than the mean, μ, of the set $\{s_{1+W/2}, \ldots, s_{N-W/2}\}$. The mid-point of each spike is collected, to form a subset of $\mathcal{T} = \{t_1, \ldots, t_N\}$ of candidate TPs. This set is reduced further by removing any candidate TPs for which the turning angle is below a certain threshold, θ_{thresh} (see Supplementary Appendix A for details). This procedure results in a set $\{t_{c_1}, \ldots, t_{c_n}\} \subset \mathcal{T}$ of *inferred TPs*.

Code for the complete algorithm is given in the Supplementary Information, as the `R` script `find_turnpoints.R` and the `Python` script `find_turnpoints.py`. Supplementary Appendix B explains how to modify and run the `R` code. Both programmes have the same function and the user can choose whichever language is more convenient.

2.2 Simulated data

To test the efficacy of this algorithm at picking out turning angles, we construct a collection of simulated trajectories. Each trajectory consists of $72,000$ data points, which can be viewed, for example, as a 30 minute path collected at a resolution of 40Hz, or a four-hour path collected at 5Hz. The actual heading of the animal at time t is denoted by μ_t.

We assume that the times between successive TPs are drawn from an exponential distribution with mean η. For our simulations, $\eta = 1,200$ time-steps. Turning angles are drawn randomly and uniformly from the set $[-\pi, -\phi_{\text{thresh}}) \cup (\phi_{\text{thresh}}, \pi)$, so that 'turns' are always greater than a threshold value, ϕ_{thresh}. The set of times at which the simulated animal makes a turn is denoted by $\{T_1, \ldots, T_m\}$. Our choice of $\eta = 1,200$ and a trajectory of length $72,000$ roughly mimics 30 minutes of oryx data, collected at 40Hz, turning on average every 30 seconds.

Because real data contains noise, we do not record the actual headings μ_t. Rather we simulate 'observed' headings, h_t, drawn from a von Mises distribution with mean μ_t and concentration parameter κ. Therefore the resulting path is a sequence of straight-line segments with noise added, interspersed with turns of greater than ϕ_{thresh}. For our analysis, we set $\phi_{\text{thresh}} = 30°$.

We construct simulated trajectories for a variety of values of κ and run each simulated trajectory through our inference algorithm for a variety of values of W and θ_{thresh}. For each trajectory, to determine how close the inferred set of TPs, $\{t_{c_1}, \ldots, t_{c_n}\}$, is to the actual set, $\{T_1, \ldots, T_m\}$, we calculate a True Positive Rate (TPR) and a False Positive Rate (FPR) using the following procedure. We split the path into windows of size W. If a window contains a true TP (i.e. one of $T_1, \ldots, T_m$) then this window is considered a *True Condition*, otherwise it

is a *False Condition*. If the window corresponding to a True Condition (resp. False Condition) contains one of the values $\{t_{c_1}, \ldots, t_{c_n}\}$ then it is a *True Positive* (resp. *False Positive*). Then the TPR (resp. FPR) is the number of true positives (resp. false positives) divided by the number of true conditions (resp. false conditions). Using the window in this way means that we accept as "True Positives" inferred TPs that are very close to real TPs (i.e. within W time-steps), but they do not have to be exactly the same points. Calculating (TPR,FPR) pairs for a variety of values of W and θ_{thresh} enables us to construct a receiver operating characteristic (ROC) curve for each value of κ (Brown and Davis, 2006).

We compare each ROC curve to the corresponding curve obtained by applying a previous turning-point algorithm, introduced by Turchin et al. (1991), to each path. Turchin's algorithm determines a turning point by iterating through a time series of *locations* (rather than headings), $x_0, ..., x_K$. If the locations $x_0, \ldots, x_{k-1}$ are all within a distance of ϵ from the straight line between x_0 and x_{k-1}, but some of the locations $x_0, \ldots, x_k$ are at a distance *greater* than ϵ from the straight line between x_0 and x_k, then the algorithm says that x_{k-1} is the first TP. Other TPs are constructed iteratively (for full details, see Turchin et al. (1991); Turchin (1998)).

For a given simulated trajectory, to compute the associated ROC curve for Turchin's algorithm, we vary ϵ and calculate each TPR- and FPR-value. One would expect low ϵ to give many TPs, so produce high values for both FPR and TPR. On the other hand, a high value of ϵ might be expected to produce low FPR and TPR. We also compare our method to a more recent method of Codling and Plank (2011) (see Supplementary Appendix D).

2.3 Case study on oryx movement

To demonstrate the efficacy of our algorithm on a real dataset, we use high-resolution magnetometer data of oryx living in Mahazat as-Sayd, a protected area located in west-central Saudi Arabia (28°15 N, 41°40E). The area consists of open steppe desert and is characterised by arid climate with hot summers, mild winters and low rainfall (Ostrowski et al., 2003). Vegetation is sparse, and predominated by perennial grasses and sporadically distributed small Acacia trees

(Mandaville, 1990).

The six oryx used in this study were captured during February 2015. After capture, they were fitted with loggers containing tri-axial accelerometers and tri-axial magnetometers (Daily Diary units, Wildbyte Technologies Ltd., Swansea, UK) which were set to record for 10 days at 40Hz in each channel. Each oryx was fitted with two daily diary units. One unit was glued to the head of the animal, behind the horns, using quick-set epoxy resin, and the other was fixed using cable ties and adhesive tape to a collar around the animals neck. Data for this study were taken from the magnetometer fitted to the neck, so that the headings represent the trajectory of the animal, rather than the direction it is facing.

Following logger deployment, animals were allowed to recover in an outside enclosure (25×25m) for approximately eight hours after which they were released into the larger enclosure (2×1km). For this study, we examine a sample path in the larger enclosure for each of the six oryx. These paths have varying lengths, the shortest is 1 hour ($\sim 140,000$ headings) and the longest is 2 hours 15 minutes ($\sim 320,000$ headings; see Supplementary Table ST1).

For real trajectories, analysis of TPR and FPR is not possible, since we do not have knowledge of the 'true' turning-points. Instead, to assess how good a proposed set of TPs is, we construct a path of straight-line segments between each pair of consecutive TPs. We compare this piecewise-linear model with the path given by the data, assuming that the animal is moving at constant speed, v (chosen arbitrarily). This latter path is given by a collection of points $\mathbf{x}(t_1), \ldots, \mathbf{x}(t_N)$, where $\mathbf{x}(t_i) = (x(t_i), y(t_i))$ is a 2D vector for each $i \in \{1, \ldots, N\}$, $\mathbf{x}(t_1) = (0, 0)$, and

$$\begin{aligned} x(t_i) &= \sum_{j=1}^{i-1} v(t_{j+1} - t_j) \cos(h_j), \\ y(t_i) &= \sum_{j=1}^{i-1} v(t_{j+1} - t_j) \sin(h_j). \end{aligned} \tag{2}$$

For a given set of inferred TPs, $\{t_{c_1}, \ldots, t_{c_n}\}$, the model path is

$$\mathbf{m}(t_i) = \mathbf{x}(t_{c_k}) + \frac{t_i - t_{c_k}}{t_{c_{k+1}} - t_{c_k}}[\mathbf{x}(t_{c_{k+1}}) - \mathbf{x}(t_{c_k})] + \xi_t, \quad \text{for } t_i \in [t_{c_k}, t_{c_{k+1}}], \tag{3}$$

where $\xi_t \sim N(\mathbf{0}, \sigma^2)$ is a random variable from a Normal distribution with zero mean and covariance matrix $\sigma^2 I$, where I is the two-dimensional identity matrix.

Note that, if we were to have a data set containing the speed at any point in time, the assumption that v is constant could be dropped and the actual speeds used instead. Furthermore, if we were to have locational data rather than just headings, we could use the measured locations as $(x(t_i), y(t_i))$ rather than constructing them using Equation (2). For the oryx data we do not have such information. However, if any future study contains locational (or positional) information at a high frequency – e.g. from dead-reckoning (Wilson et al., 2008) – then these locations should be used directly to construct a piecewise-linear model similar to Equation (3).

An estimate for the standard deviation, σ, can be calculated empirically, as follows. Let $\mathbf{d}(t_i) = \mathbf{x}(t_i) - \langle \mathbf{m}(t_i) \rangle$ for each $i \in \{1, \ldots, N\}$, where $\langle \mathbf{m}(t_i) \rangle$ is the mean of $\mathbf{m}(t_i)$. Since $\langle \mathbf{m}(t_i) \rangle$ is the point on a straight line between inferred turning points corresponding to $\mathbf{x}(t_i)$, $\mathbf{d}(t_i)$ is the deviation of the measured location from the corresponding location on this straight line (i.e. the residual). Then σ is estimated to be the standard deviation of the set $\{\mathbf{d}(t_1), \ldots, \mathbf{d}(t_N)\}$. A smaller σ indicates a better fit of the model to the data. Since σ is dependent on our (arbitrary) choice of animal speed, we define a *normalised standard deviation*, $\bar{\sigma} = \sigma / \langle l_i \rangle$, where $\langle l_i \rangle$ is the mean of the step lengths $l_i = |\mathbf{x}(t_{c_k}) - \mathbf{x}(t_{c_{k-1}})|$. Then $\bar{\sigma}$ is a dimensionless quantity, independent of v.

For analysis of the oryx data, we choose values for W and θ_{thresh} by examining (a) those that perform well on simulated data (i.e. low FPR and high TPF), (b) those that are biologically justifiable (i.e. expert opinion). We also construct videos of the trajectories, with the turnpoints super-imposed, so one can visually inspect whether the estimations of TPs look reasonable to the human eye. This aids in determining whether our choice of W and θ_{thresh} give the correct

information.

We use the oryx data to compare our algorithm with the output of the `Segmentor3isBack` package. `Segmentor3isBack` is a general-use programme that segments data-streams into K segments, where K is fixed (and user-defined). The package can also find the theoretical optimal value of K for fitting a trajectory of straight-line segments interspersed with break-points. We compare the time it takes to run the respective algorithms, as well as the resulting $\bar{\sigma}$ values, when K is set to be equal to the number of segments given by our algorithm. For this, we fix $W = 40$ and $\theta_{\text{thresh}} = 30°$.

We also compare our algorithm to Turchin's algorithm, where ϵ is set so that resulting number of segments is equal to that given by our algorithm. Turchin's algorithm has to be applied to the reconstructed path (Equation 2) rather than the raw headings. It also defines turns in such a way as to minimise the distance between the model path (Equation 3) and the reconstructed one (Equation 2. It can thus be viewed as providing an rough estimate of the minimum $\bar{\sigma}$ that may be attainable. We also examined the effect of pre-processing our data by smoothing-out possible noise arising from the animal's gait or minor obstacle avoidance, before running it through out algorithm. This provides a prior smoothing before the implicit smoothing given by choice of window size, W. Details are given in Supplementary Appendix C.

3 Results

3.1 Simulated data: comparison with previous approaches

Fig. 2 shows three simulated trajectories, with an increasing level of noise from left to right. The ROC curves (Panels j-l) indicate that the method proposed here finds the TPs with significantly better accuracy than the method of Turchin et al. (1991). Indeed, for the example where the SD in the error of the heading measurements is only $\pm 8.1°$, our method had a TPR of 1 and FPR of 0, meaning it caught all of the true TPs and did not falsely identify any

TPs. This suggests that if an animal really is moving in straight-lines separated by distinct turns, then our method will be extremely accurate at picking these up, as long as the SD in the heading measurements is not too great (i.e. of the order of $< 10°$). The method of Codling and Plank (2011) performed worst of the three and is probably only suitable where data is much lower resolution (see Supplementary Appendix D).

3.2 Oryx data

To identify turns in the oryx data, we found that a window size of $W = 40$ data points and $\theta_{\text{thresh}} = 30°$ gave accurate results for determining both broad- and fine-scale movement decisions. Since data were taken 40 times per second, this means that we are only integrating-out behavioural features that occur on a subsecond resolution, which are likely to be minimal-to-nonexistent. Fig. 3a shows an example of an oryx path with these inferred turns superimposed. At first glance, it appears as if there are a number of places where turns are identified where they do not appear to be present. However, by zooming-in, we observe that the algorithm is actually correctly identifying very fine-scale movements correctly (see inset of Fig. 3a).

Depending on the biological question being sought, a user may not be interested in very fine-scale movements, so may wish to smooth out behaviour over a longer time-interval. For example, we also used a window size of $W = 200$, corresponding to five seconds of movement, to analyse the same oryx path as in Fig. 3b. Here, the very fine-scale movements are integrated out, leaving a much smaller set of TPs (155 compared with 498). Videos of the trajectory of Oryx 1 with the inferred turning points for $W = 40$ and $W = 200$ are given in Supplementary Videos SV1 (cpsv1.mp4) and SV2 (cpsv2.mp4), respectively. Pre-processing data using subsampling or smoothing had almost no effect on the inference (Supplementary Appendix C).

Table 1 summarises the number of TPs inferred for each of the six oryx paths, using $\theta_{\text{thresh}} = 30°$ and $W \in \{40, 200\}$, together with the normalised standard deviation, $\bar{\sigma}$ of the data from the piecewise-linear model given by Equation (3). Observe that this normalised standard deviation is similar for both $W = 40$ and $W = 200$. The reason for this is that,

Table 1. Application to oryx data. The first column is the oryx identifier. The second (resp. fourth) gives the normalised standard deviation of the model from the data for a window size of $W = 40$ (resp. $W = 200$) data points, representing 1 second (resp. 5 seconds) of movement. The third (resp. fifth) gives the number of inferred turning points (TPs) for a window size of $W = 40$ (resp. $W = 200$) data points.

Oryx ID	$\bar{\sigma}$ ($W = 40$)	No. TPs ($W = 40$)	$\bar{\sigma}$ ($W = 200$)	No. TPs ($W = 200$)
1	0.0601	498	0.0612	155
2	0.0783	892	0.0792	261
3	0.381	557	0.508	153
4	0.477	863	0.180	217
5	0.176	639	0.187	183
6	0.247	929	0.198	237

although the step lengths are longer for the piecewise-linear models with fewer TPs ($W = 200$), small-scale turns are treated as noise rather than signal, thus increasing the amount of error proportionately.

Comparing our algorithm with `Segmentor3isBack`, we see that the latter tends to be about 10^3 times slower (e.g. 46 minutes compared to 3.6 seconds; see Supplementary Table ST1 for precise figures). The resulting path of straight lines and turns is a marginally better fit in five of the six cases (Supplementary Table ST1), which is to be expected, since `Segmentor3isBack` is designed to find the theoretical best-fit path. However, the difference tends to be minor, both by comparing $\bar{\sigma}$-values and by visually inspecting the paths (Supplementary Figure SF4).

Comparison with Turchin's algorithm, applied to the reconstructed path (Equation 2), reveals that Turchin's algorithm is 1-2 orders of magnitude slower (e.g. 220 seconds compared to 3.6 seconds; see Supplementary Table ST2 for precise figures). Turchin's algorithm generally results in a lower $\bar{\sigma}$. This is to be expected as Turchin's method defines turns as places where there is a deviation from a straight-line of more than a fixed value, so implicitly seeks to minimise $\bar{\sigma}$. However, our simulation analysis reveals that this is not such an accurate method for determining where turns have actually occurred, as it is more likely to misdetect noise as signal than our approach (Fig. 2). Therefore the resulting inferred set of turning points is not as reliable as our algorithm, even though the constructed piecewise linear path may turn out

to have a slightly better fit.

4 Discussion

We have described a fast, accurate algorithm for detecting turning-points in animal movement data, particularly tailored for use with very high-resolution data. Given a path of straight-moves and turns, where headings have been measured to within an accuracy of within $\pm 8.1^\circ$ standard deviation, the algorithm succeeds in detecting all turning points, without falsely detecting any (Fig. 2). If the accuracy is only $\pm 19.6^\circ$, the algorithm was still able to identify 56 of 59 turnings points, whilst misclassifying 8 non-turns as turning points. Since many modern measuring devices, such as magnetometers, have an accuracy within $\pm 5^\circ$ (Li et al., 2006), this suggests our algorithm is well-suited to identifying turning-points in such data (as long as the tag is attached well and does not shift location on the animal significantly).

This accuracy compares well with previous methods. Perhaps the most oft-used in movement ecology has been that of Turchin et al. (1991), which ours markedly improves upon (Fig. 2). A more sophisticated method, imported from literature on statistics and DNA segmentation (Cleynen et al., 2014), does a reasonable job on real data (Supplementary Table ST1, Supplementary Figure SF4) but is around three orders of magnitude slower than our method (Supplementary Table ST1). Indeed, the speed of our algorithm is a very important feature. Datasets are becoming ever larger, so having fast algorithms without significant scaling problems is very important. Ours will analyse hundreds of thousands of data points in a few seconds on an ordinary desktop and scales linearly. Therefore, we expect that even tracks of a billion locations (40Hz for a year) would be analysable in only a few hours.

Our method complements existing research in analysis of behavioural changepoints in animal paths, recently reviewed by Edelhoff et al. (2016). These methods look at movement paths at a broader scale, segmenting them into sections corresponding to different behavioural modes. Edelhoff et al. (2016) explained how this analysis can be broken down into four stages [see Fig. 1 from Edelhoff et al. (2016)], with the third stage ostensibly very similar to the

sort of turning-point analysis described here. However, a detailed look reveals that the papers that are referenced regarding this third stage are, in fact, seeking answers to issues that are somewhat different to the aims of this paper, which we explain in the next two paragraphs. Our contention will be that the method presented here is a sub-step prior to Edelhoff *et al.*'s third step, required when data is very high resolution (a case not considered in Edelhoff *et al.*).

Several methods for behavioural changepoint analysis (BCPA) have been proposed in the literature. Many of them begin with a description of movement in terms of summary statistics. For example, Gurarie et al. (2009) gives an algorithm for determining significant changes in persistence velocity and turning velocity. Similar ideas were given a more general and theoretical treatment by Buchin et al. (2011). Nams (2014) generalises BCPA by developing a technique for detecting behavioural changepoints that can make use of a wide variety of summary statistics, and also clusters the resulting path-segments into distinct behavioural states. Postlethwaite et al. (2013) proposes a 'straightness index' for rapid inference of behavioural states. Gurarie et al. (2016) summarises and compares a variety of methods for detecting behavioural changes.

However, all such behavioural changepoint techniques require that the path be already described using some sort of summary statistic (e.g. velocity, tortuousity, turning angle distribution etc.). Our paper provides a method to infer specific summary statistics (i.e. step lengths and turning angles) from big, high-resolution datasets, thus enabling existing behavioural changepoint analysis techniques to be used with high-resolution data. We thus anticipate that the output of our algorithm could be effectively used as an input to BCPA and similar methods.

Our method, based on the circular statistics of headings, has some mathematical similarities with certain methods of deriving toruousity in movement paths (Benhamou, 2004). If the underlying distribution of headings comes from a wrapped normal distribution then the SCSD is an unbiased estimator of the variance of the underlying (unwrapped) normal distribution (Mardia, 2014). The mean of the cosine of a wrapped normal distribution is then $c = \exp(-\text{SCSD}/2)$

(Mardia and Jupp, 2009). The quantity c has been applied to turning angles of animal paths to measure the tortuousity of such paths, since it interpolates between 0 for an uncorrelated random walk to 1 for ballistic movement (Bovet and Benhamou, 1988). Indeed, it has been used, combined with a sliding window, to detect changes in the behavioural mode of animals (Benhamou, 2004). So there are some strong similarities between this approach and ours. The main differences are that the existing studies using c have been concerned with behavioural changepoints rather than (smaller scale) turning points, and generally applied to turning angles rather than headings (since the underlying questions are different). Also, the wrapped normal assumption that links the two is not so easy to justify when applied to our scenario, especially near turning points.

The study of Byrne et al. (2009) also examines changes in behaviour, but this time by explicitly looking for a change in direction. The aim was to identify the points at which an animal decides to move towards a particular location. The method compares the sum of the lengths of two straight line segments $|\mathbf{x}_{n-1} - \mathbf{x}_n| + |\mathbf{x}_n - \mathbf{x}_{n+1}|$ with the resultant length $|\mathbf{x}_{n-1} - \mathbf{x}_{n+1}|$ to infer a change in direction if the latter is much smaller than the former.

Whilst this method asks a similar question to the one examined here, in fact it is not designed to pick up every turn, but just those that indicate a decision to move to a specific location. Indeed, it quite deliberately ignores small, temporary changes in direction, as Fig. 4 from Byrne et al. (2009) demonstrates. Our algorithm, on the other hand, does attempt to detect every change in direction, however temporary it is. However, it is possible for the user to factor-out temporary changes by choosing a large window size, W. Ultimately, the choice of whether it is best to use our algorithm or the one from Byrne et al. (2009) will depend on the specific biological question, and the summary statistics desired to answer it (notwithstanding additional issues regarding computational speed for big data sets).

In general, the choice of both W and θ_{thresh} depends on various factors and a combination of statistical tests and expert knowledge will be required in order for this be set appropriately. Our simulation analysis indicates that there is an optimal W and θ_{thresh} for a given simulation

scenario, defined by the point at the upper-left-most extreme of the ROC curve (see Fig. 2j-l). However, for real data it is not possible to construct such a ROC curve and find the actual optimum. Instead we recommend calculating the variation of the real trajectory from a piecewise-linear model trajectory with turns at the inferred turning points. Such a trajectory is described in Equation (3). Furthermore, we give a dimensionless quantity, denoted by $\bar{\sigma}$, for testing this fit. To choose W and θ_{thresh}, we recommend, in the first instance, running our algorithm over a range of values and calculating $\bar{\sigma}$ for each.

Although lower values of $\bar{\sigma}$ indicate a better fit, the correct choice of W and θ_{thresh} also depends upon the biological properties of the study species and the underlying scientific questions. This is where expert opinion becomes important, and blindly picking the W and θ_{thresh} that minimise $\bar{\sigma}$ may not always be the best option. In particular, the turn radii of the species is an important quantity. The minimum turn radius of an animal depends partly on its movement speed, with faster moving individuals (or species) tending to have greater turn radii (Alexander, 2002*a*), with this condition generally holding whether the animal in question is aerial (Thomas, 1996), terrestrial (Alexander, 2002*b*) or aquatic (but see Blake et al. (1995) and references therein), although values differ in the different media. In particular, it is worth noting that terrestrial mammals, such as the oryx used in this work, may turn through 90° in less than 1s whereas, because a flying bird has a turn radius that is proportional to the flight speed squared (Thomas, 1996), a similar 90° turn by a large gliding bird such as a condor (*Vultur gryphus*) may take several seconds during which time the bird may have travelled 50m (McGahan, 1973).

In addition to this, there are extrinsic factors that may mean an animal moves in a curve rather than a straight line between successive decisions to change direction. For example, topography could affect a terrestrial animal, and water (resp. air) currents will affect aquatic (resp. airborne) animals. Therefore, when finding turning-points in such data, it is necessary to factor-out such extrinsic effects. (Note that the oryx studied here are unlikely to be largely affected by such factors, as they roam on relatively flat and open terrain.) If, once all these

factors are accounted for, an animal's path is curvilinear, rather than consisting of straight-lines and turns, then our algorithm is simply inappropriate for analysing the path and should not be used.

If there is noise in the data arising from specific known artifacts, such as effects of rocky terrain or animal gait, then it may be beneficial to pre-process the data prior to analysis so as to smooth-out this noise. Some possible pre-processing methods are given in Supplementary Appendix C. We recommend users test for such noise, ideally by examining short paths where the animal has been directly observed to go in a straight line. If this is not possible, attaching the magnetometer to a human in the same terrain where the animal resides can give an idea (albeit imperfect) of the noise due to an uneven terrain. Similarly, we recommend that users obtain an idea of the noise inherent in the magnetometer by leaving it immobile at a fixed heading for some time. If there any of these types of noise are either large or autocorrelated, then it may be beneficial to examine the effect of pre-processing the data. For the oryx examined here, however, such pre-processing had almost no effect on the inference (Supplementary Appendix C).

Our method makes an implicit choice to define a candidate turn as a point at which the SCSD goes above the global mean. Whilst this choice appears to work adequately in the situations studied here, it is not the only possible way to define a turn. For example, one could examine the *cumulative* SCSD and look for sharp changes in the resulting time series, using the methods described by Knell and Codling (2012). There, the authors examined how the cumulative sum (CUSUM) of any summary statistic (not necessarily SCSD) will change sharply over time when the behaviour changes (in the context of our study, this 'behavioural change' would be between straight-moving and turning). However, the CUSUM method also relies on an arbitrary choice of a parameter [labelled ε by Knell and Codling (2012)] to determine where such sharp changes occur in the time series. Although the authors demonstrate a method for calculating an optimal ε in certain circumstances, it is not clear whether it would always be possible to derive such an optimum in any situation. Therefore, whilst a CUSUM approach

to SCSD may sometimes be a useful option for the user to bear in mind, it may also end up simply replacing one arbitrary choice with another.

In summary, our algorithm is a quick and accurate method for splitting up long streams of ultra high resolution animal movement data into straight-line segments and turns. The output of such segmentation can then be used to detect behavioural features using the myriad techniques that require step-and-turn descriptions, such as step selection analysis, behavioural changepoint analysis, state space models, and more. In particular, step selection analysis (SSA) would greatly benefit from an approach whereby the 'steps', which typically mean a movement from one measured location to the next, are replaced with the more behaviourally-driven 'moves' from one turning point to the next. SSA seeks to understand whether a movement along one straight-line path is preferable to another and how that is correlated to environmental covariates. Evidently, this inference will be improved if the animal's actual movement from one point to the next well-approximates a straight line. So replacing 'steps' with 'moves' seems to be the correct way forward.

With some of the other aforementioned techniques, such as behavioural changepoint analysis, it is less clear whether 'steps' or 'moves' would be more appropriate [to borrow terminology from Turchin (1998), Section 5.2]. If a technique uses turning angles as a summary statistic for analysing behaviour, it would seem more appropriate to use 'moves' as the angles would correspond to actual turns by the animal, which may be energetically costly (Wilson et al., 2013). For example, the calculations of persistence velocity and turning velocity in Gurarie et al. (2009) would be improved by using 'moves'. However, if the analysis relies upon regular sampling of animal locations then one may have to use 'steps'. For example, techniques such as Morales et al. (2004); Beyer et al. (2013) rely on step-length distributions between locations gathered (roughly) regularly in time. These would need to be carefully adapted before use with a sequence of 'moves' of different time-periods. That said, if such an adaption can be made, a switch from 'step length distribution' to 'move length distribution' would be possible within these frameworks, and may make them more behaviourally-grounded. In conclusion, given its

potential for use to improve a broad range of existing techniques, our algorithm should serve as an important tool for making sense of the type big data increasingly available to movement ecologists.

Acknowledgements

The data-gathering part of this project was funded by the National Plan for Science, Technology and Innovation (MAARIFAH), King Abdulaziz City for Science and Technology, Kingdom of Saudi Arabia, Award Number (11-ENV1918-02) and the Deanship of Scientific Research at the King Saud University through Vice Deanship of Research Chairs. Ethical clearance for the data-gathering was obtained from the University of the Witwatersrand Animal Ethics Committee (clearance certificate number 2014/53/D). Permission to work in the field was granted by the President of the Saudi Wildlife Authority. JRP acknowledges support from the National Environmental Research Council (NERC) grant NE/R001669/1. The authors thank two anonymous reviewers and an associate editor for comments that have helped improve the manuscript.

Author Contributions

JRP, LB, RPW conceived and designed the research; JRP, LB performed the research; LB, DMS, NCB, AA, RPW provided data; JRP led the writing of the manuscript. All authors contributed critically to the drafts and gave final approval for publication.

Data Accessibility

Data used in this manuscript will be archived on FigShare after the manuscript has been accepted for publication.

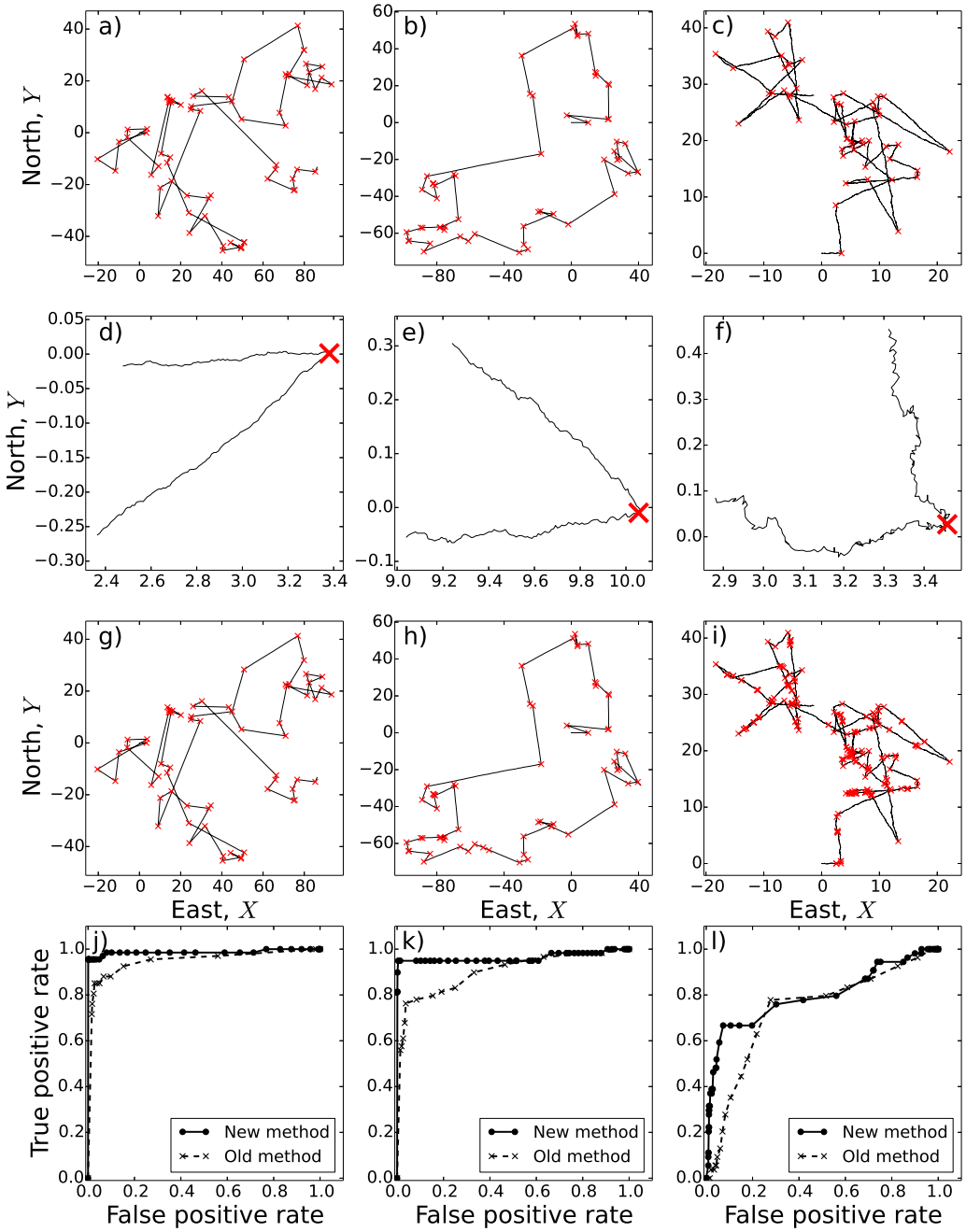

Fig. 2. Simulated paths. The top panels (a-c) give three simulated trajectories with increasing amounts of noise from left to right. Specifically, panel (a) has $\kappa = 50$ so the standard deviation (SD) in the heading is 8.1°; panel (b) has $\kappa = 10$, corresponding to an SD of 18.6°; panel (c) has $\kappa = 1$ so SD= 72.6°. The actual TPs are superimposed on the trajectories in panels (a-c) as crosses. Panels (d-f) zoom in on panels (a-c) respectively around the first turning point, giving a better visual impression of the noise in the data. Panels (g-i) show the same trajectories as (a-c) respectively, but this time the red crosses show inferred TPs using the inference method described in the Main Text. Panels (j-l) show ROC curves, corresponding to the trajectories in (a-c) respectively, for both the method introduced here (dots and solid curves) and an older method due to Turchin et al. (1991) (crosses and dashed curves).

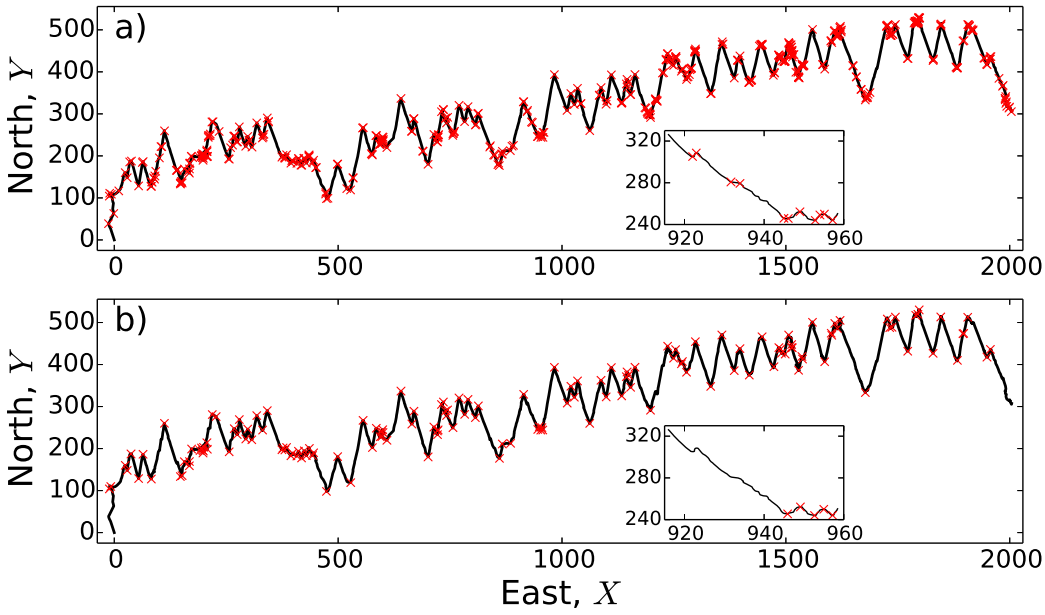

Fig. 3. Example oryx path. Both panels show the path of a single oryx (ID=1 in Table 1). In Panel (a) the red crosses denote the inferred turning points (TPs) using a window size $W = 40$ (corresponding to 1 second of movement) and a turning threshold angle of $\theta_{\text{thresh}} = 30°$. The inset zooms in on a fragment of the path, to demonstrate the very small-scale turns that are revealed by this analysis, alongside broader-scale turning decisions. In Panel (b), the TPs are inferred using a window size of $W = 200$ (5 seconds of movement). The very fine-scale turns are now smoothed-out (inset, Panel b), which allows the user to focus on broader-scale patterns.

References

Alexander, R. M. 2002*a*. The Merits and Implications of Travel by Swimming, Flight and Running for Animals of Different Sizes. Integrative and Comparative Biology, **42**:1060–1064.

Alexander, R. M. 2002*b*. Stability and manoeuvrability of terrestrial vertebrates. Integrative and Comparative Biology, **42**:158–164.

Avgar, T., J. R. Potts, M. A. Lewis, and M. S. Boyce. 2016. Integrated step selection analysis: bridging the gap between resource selection and animal movement. Methods in Ecology and Evolution, **7**:619–630.

Benhamou, S. 2004. How to reliably estimate the tortuosity of an animal's path:: straightness, sinuosity, or fractal dimension? Journal of Theoretical Biology, **229**:209–220.

Berens, P. 2009. CircStat: a MATLAB toolbox for circular statistics. Journal of Statistical Software, **31**:1–21.

Beyer, H. L., J. M. Morales, D. Murray, and M.-J. Fortin. 2013. The effectiveness of Bayesian state-space models for estimating behavioural states from movement paths. Methods in Ecology and Evolution, **4**:433–441.

Bidder, O., J. Walker, M. Jones, M. Holton, P. Urge, D. Scantlebury, N. Marks, E. Magowan, I. Maguire, and R. Wilson. 2015. Step by step: reconstruction of terrestrial animal movement paths by dead-reckoning. Movement Ecology, **3**:23.

Blake, R., L. Chatters, and P. Domenici. 1995. Turning radius of yellowfin tuna (Thunnus albacares) in unsteady swimming manoeuvres. Journal of fish biology, **46**:536–538.

Bovet, P. and S. Benhamou. 1988. Spatial analysis of animals' movements using a correlated random walk model. Journal of Theoretical Biology, **131**:419–433.

Brown, C. D. and H. T. Davis. 2006. Receiver operating characteristics curves and related decision measures: A tutorial. Chemometrics and Intelligent Laboratory Systems, **80**:24–38.

533 Brown, D. D., R. Kays, M. Wikelski, R. Wilson, and A. P. Klimley. 2013. Observing the
534 unwatchable through acceleration logging of animal behavior. Animal Biotelemetry, **1**:20.

535 Buchin, M., A. Driemel, M. Van Kreveld, and V. Sacristán. 2011. Segmenting trajectories:
536 A framework and algorithms using spatiotemporal criteria. Journal of Spatial Information
537 Science, **2011**:33–63.

538 Byrne, R., R. Noser, L. Bates, and P. Jupp. 2009. How did they get here from there? Detecting
539 changes of direction in terrestrial ranging. Animal Behaviour, **77**:619–631.

540 Cleynen, A., M. Koskas, E. Lebarbier, G. Rigaill, and S. Robin. 2014. Segmentor3IsBack: an R
541 package for the fast and exact segmentation of Seq-data. Algorithms for Molecular Biology,
542 **9**:6.

543 Codling, E. A. and M. J. Plank. 2011. Turn designation, sampling rate and the misidentification
544 of power laws in movement path data using maximum likelihood estimates. Theoretical
545 Ecology, **4**:397–406.

546 Codling, E. A., M. J. Plank, and S. Benhamou. 2008. Random walk models in biology. Journal
547 of the Royal Society Interface, **5**:813–834.

548 Edelhoff, H., J. Signer, and N. Balkenhol. 2016. Path segmentation for beginners: an overview
549 of current methods for detecting changes in animal movement patterns. Movement Ecology,
550 **4**:21.

551 Erdman, C. and J. W. Emerson. 2008. A fast Bayesian change point analysis for the segmen-
552 tation of microarray data. Bioinformatics, **24**:2143–2148.

553 Forester, J., H. Im, and P. Rathouz. 2009. Accounting for animal movement in estimation of
554 resource selection functions: sampling and data analysis. Ecology, **90**:3554–3565.

555 Fortin, D., H. Beyer, M. Boyce, D. Smith, T. Duchesne, and J. Mao. 2005. Wolves influence

556 elk movements: Behavior shapes a trophic cascade in Yellowstone National Park. Ecology,
557 **86**:1320–1330.

558 Franke, J., C. Kirch, and J. T. Kamgaing. 2012. Changepoints in times series of counts. Journal
559 of Time Series Analysis, **33**:757–770.

560 Gurarie, E., R. D. Andrews, and K. L. Laidre. 2009. A novel method for identifying behavioural
561 changes in animal movement data. Ecology Letters, **12**:395–408.

562 Gurarie, E., C. Bracis, M. Delgado, T. D. Meckley, I. Kojola, and C. M. Wagner. 2016. What is
563 the animal doing? Tools for exploring behavioural structure in animal movements. Journal
564 of Animal Ecology, **85**:69–84.

565 Hays, G. C., L. C. Ferreira, A. M. Sequeira, M. G. Meekan, C. M. Duarte, H. Bailey, F. Bailleul,
566 W. D. Bowen, M. J. Caley, D. P. Costa, et al. 2016. Key questions in marine megafauna
567 movement ecology. Trends in Ecology & Evolution, **31**:463–475.

568 Hocking, T. D., G. Schleiermacher, I. Janoueix-Lerosey, V. Boeva, J. Cappo, O. Delattre,
569 F. Bach, and J.-P. Vert. 2013. Learning smoothing models of copy number profiles using
570 breakpoint annotations. BMC Bioinformatics, **14**:164.

571 Hurford, A. 2009. GPS measurement error gives rise to spurious 180 turning angles and strong
572 directional biases in animal movement data. PLoS One, **4**:e5632.

573 Jerde, C. L. and D. R. Visscher. 2005. GPS measurement error influences on movement model
574 parameterization. Ecological Applications, **15**:806–810.

575 Johnson, C. J., D. C. Heard, and K. L. Parker. 2002. Expectations and realities of GPS animal
576 location collars: results of three years in the field. Wildlife Biology, **8**:153–159.

577 Jonsen, I. D., J. M. Flemming, and R. A. Myers. 2005. Robust state–space modeling of animal
578 movement data. Ecology, **86**:2874–2880.

579 Kareiva, P. and N. Shigesada. 1983. Analyzing insect movement as a correlated random walk.
580 Oecologia, **56**:234–238.

581 Kays, R., M. C. Crofoot, W. Jetz, and M. Wikelski. 2015. Terrestrial animal tracking as an
582 eye on life and planet. Science, **348**:aaa2478.

583 Knell, A. S. and E. A. Codling. 2012. Classifying area-restricted search (ARS) using a partial
584 sum approach. Theoretical Ecology, **5**:325–339.

585 Li, Y., A. Dempster, B. Li, J. Wang, and C. Rizos. 2006. A low-cost attitude heading reference
586 system by combination of GPS and magnetometers and MEMS inertial sensors for mobile
587 applications. Journal of Global Positioning Systems, **1**:0.

588 Mandaville, J. P. 1990. Flora of Eastern Saudi Arabia. London: Kegan Paul Int.

589 Mardia, K. V. 2014. Statistics of directional data. Academic press.

590 Mardia, K. V. and P. E. Jupp. 2009. Directional statistics, volume 494. John Wiley & Sons.

591 McClintock, B. T., J. M. London, M. F. Cameron, and P. L. Boveng. 2015. Modelling animal
592 movement using the Argos satellite telemetry location error ellipse. Methods in Ecology and
593 Evolution, **6**:266–277.

594 McGahan, J. 1973. Gliding flight of the Andean condor in nature. Journal of Experimental
595 Biology, **58**:225–237.

596 Morales, J. M., D. T. Haydon, J. Frair, K. E. Holsinger, and J. M. Fryxell. 2004. Extract-
597 ing more out of relocation data: building movement models as mixtures of random walks.
598 Ecology, **85**:2436–2445.

599 Nams, V. O. 2014. Combining animal movements and behavioural data to detect behavioural
600 states. Ecology Letters, **17**:1228–1237.

Nathan, R., W. M. Getz, E. Revilla, M. Holyoak, R. Kadmon, D. Saltz, and P. E. Smouse. 2008. A movement ecology paradigm for unifying organismal movement research. Proceedings of the National Academy of Sciences, **105**:19052–19059.

Noda, T., Y. Kawabata, N. Arai, H. Mitamura, and S. Watanabe. 2014. Animal-mounted gyroscope/accelerometer/magnetometer: In situ measurement of the movement performance of fast-start behaviour in fish. Journal of Experimental Marine Biology and Ecology, **451**:55–68.

Ostrowski, S., J. B. Williams, and K. Ismael. 2003. Heterothermy and the water economy of free-living Arabian oryx (Oryx leucoryx). Journal of Experimental Biology, **206**:1471–1478.

Parton, A., P. G. Blackwell, and A. Skarin. 2016. Bayesian inference for continuous time animal movement based on steps and turns. In International Conference on Bayesian Statistics in Action, pages 223–230. Springer.

Patterson, T. A., L. Thomas, C. Wilcox, O. Ovaskainen, and J. Matthiopoulos. 2008. State–space models of individual animal movement. Trends in Ecology & Evolution, **23**:87–94.

Picard, F., S. Robin, M. Lavielle, C. Vaisse, and J.-J. Daudin. 2005. A statistical approach for array CGH data analysis. BMC Bioinformatics, **6**:27.

Postlethwaite, C. M., P. Brown, and T. E. Dennis. 2013. A new multi-scale measure for analysing animal movement data. Journal of Theoretical Biology, **317**:175–185.

Rhodes, J., C. McAlpine, D. Lunney, and H. Possingham. 2005. A spatially explicit habitat selection model incorporating home range behavior. Ecology, **86**:1199–1205.

Rivera, C. and G. Walther. 2013. Optimal detection of a jump in the intensity of a Poisson process or in a density with likelihood ratio statistics. Scandinavian Journal of Statistics, **40**:752–769.

624 Thomas, A. L. 1996. The flight of birds that have wings and a tail: variable geometry expands
625 the envelope of flight performance. Journal of Theoretical Biology, **183**:237–245.

626 Turchin, P. 1998. Quantitative analysis of movement: measuring and modeling population re-
627 distribution in animals and plants, volume 1. Sinauer Associates Sunderland, Massachusetts,
628 USA.

629 Turchin, P., F. Odendaal, and M. Rausher. 1991. Quantifying insect movement in the field.
630 Environmental Entomology, **20**:955–963.

631 Walker, J. S., M. W. Jones, R. S. Laramee, M. D. Holton, E. L. Shepard, H. J. Williams,
632 D. M. Scantlebury, J. M. Nikki, E. A. Magowan, I. E. Maguire, et al. 2015. Prying into the
633 intimate secrets of animal lives; software beyond hardware for comprehensive annotation in
634 Daily Diary tags. Movement Ecology, **3**:29.

635 Williams, H. J., M. D. Holton, E. L. Shepard, N. Largey, B. Norman, P. G. Ryan, O. Duriez,
636 M. Scantlebury, F. Quintana, E. A. Magowan, et al. 2017. Identification of animal movement
637 patterns using tri-axial magnetometry. Movement Ecology, **5**:6.

638 Wilmers, C. C., B. Nickel, C. M. Bryce, J. A. Smith, R. E. Wheat, and V. Yovovich. 2015. The
639 golden age of bio-logging: how animal-borne sensors are advancing the frontiers of ecology.
640 Ecology, **96**:1741–1753.

641 Wilson, R. P., I. W. Griffiths, P. A. Legg, M. I. Friswell, O. R. Bidder, L. G. Halsey, S. A.
642 Lambertucci, and E. L. C. Shepard. 2013. Turn costs change the value of animal search
643 paths. Ecol. Lett., **16**:1145–1150.

644 Wilson, R. P., E. Shepard, and N. Liebsch. 2008. Prying into the intimate details of animal
645 lives: use of a daily diary on animals. Endangered Species Research, **4**:123–137.